Effects of shear flows on nonlinear waves in excitable media

V.N. Biktashev[1,†], I.V. Biktasheva[1,†], A.V. Holden[1], M.A. Tsyganov[1,‡]
J. Brindley[2], N.A. Hill[2],

December 21, 1998

[1] *School of Biomedical Sciences and* [2] *Department of Applied Mathematics, University of Leeds, Leeds LS2 9JT, UK*
[†] *On leave from Institute for Mathematical Problems in Biology, Pushchino, Moscow region, 142292, Russia*
[‡] *Also with Institute for Theoretical and Experimental Biophysics, Pushchino, Moscow region, 142292, Russia*

shortened version: "Effects of shear flows on excitation waves"

Abstract

If an excitable medium is moving with relative shear, the waves of excitation may be broken by the motion. We consider such breaks for the case of a constant linear shear flow. The mechanisms and conditions for the breaking of solitary waves and wavetrains are essentially different: the solitary waves require the velocity gradient to exceed a certain threshold, whilst the breaking of repetitive wavetrains happens for arbitrarily small velocity gradients. Since broken waves evolve into new spiral wave sources, this leads to spatio-temporal irregularity.

Key words: frazzle gas, spiral wave, wave breakdown, excitable medium, autowave, plankton dynamics, advection, shear flow, reaction-diffusion system.

1 Introduction

Excitable medium models, in the form of partial differential equations of the reaction-diffusion type, have been used to account for nonlinear wave phenomena in many areas of biology — intracellular calcium waves, excitation in nerve, muscle and cardiac muscle, morphogenesis in the slime mold [1] and in population dynamics [2]. An excitable system responds to a small subthreshold perturbation by a graded, decremental response, and to a suprathreshold perturbation by a large amplitude pulse or pulse train; the best known example is the action potential. This threshold property is characteristic of a cubic nonlinearity, as in the FitzHugh-Nagumo equations for an excitation process E and a recovery process g

$$\begin{aligned} \frac{\partial E}{\partial t} &= c_1 E(E-a)(1-E) - g, \\ \frac{\partial g}{\partial t} &= \epsilon(c_2 E - g). \end{aligned} \tag{1}$$

In a spatially extended system the suprathreshold response is a non-decremental travelling wave or a wave train. When such a cubic nonlinearity is included in a reaction-diffusion equation

$$\begin{aligned} \frac{\partial E}{\partial t} &= c_1 E(E-a)(1-E) - g + D\nabla^2 E, \\ \frac{\partial g}{\partial t} &= \epsilon(c_2 E - g) + \delta D\nabla^2 g, \end{aligned} \tag{2}$$

in a two-dimensional medium, appropriate initial conditions can lead to a spiral wave. Such spiral waves (or scroll waves in three-dimensions) have been observed in many biological excitable media.

Truscott and Brindley have proposed that plankton dynamics may be represented by an excitable system, with the phytoplankton concentration behaving as the excitation process, and the zooplankton concentration behaving as a slower recovery variable. Just as high order cardiac excitation equations, with variables that change over many time scales, can be idealised by the FitzHugh-Nagumo system for modelling excitation processes in the heart, the temporal behaviour of plankton populations can be caricatured by a simple two or three variable system [3][4]. These models have been used to account for plankton blooms [5] and the triggering of blooms in the Ironex II experiment [6] [7]. In this case the ocean provides the medium within which the plankton dynamics evolves in time. Although plankton blooms exhibit the properties of an excitable system, propagating wave trains and spiral and scroll wave behaviour are not apparent in plankton spatio-temporal dynamics.

Cardiac muscle is another example of a moving excitable medium. Heart motion is a consequence of muscle contraction which is triggered by excitation, and excitation propagation may depend on the motion of the muscle, thus there is a mechano-electric feed-back loop. The majority of experiments on propagation of excitation in cardiac muscle are made on immobilised preparations. However, *in vivo* this feedback is present, and theoretical considerations show that motion of the muscle can significantly alter the excitation propagation patterns [8].

In this paper, we consider the effects of medium motion, represented by simple shear flows, on wave behaviours in excitable media, and show that, although a solitary wave can be stable in a shear flow, repetitive activity, including spiral wave activity, is broken down by arbitrarily small shear flows, and so spatio-temporal irregularity (a frazzle gas, or autowave turbulence) is the expected wave behaviour in a moving excitable medium.

2 Plane waves in linear shear flows

The generic reaction-diffusion system in a shear flow in the (x, y) plane can be written in the form

$$\frac{\partial u}{\partial t} = f(u) + \alpha y \frac{\partial u}{\partial x} + D\left(\frac{\partial^2 u}{\partial x^2} + \frac{\partial^2 u}{\partial y^2}\right), \tag{3}$$

where u is the column vector of reacting species, f represents the nonlinear reaction rates, D is the diffusion matrix and α is the gradient of the advection velocity, $\vec{c} \equiv (\alpha y, 0)$. We assume that, for $\alpha = 0$, the (1+1)-dimensional version of this system has solutions in the form of periodic waves, with the speed and shape determined by the period, and a unique solitary wave solution.

Consider the propagation of plane wave solutions. Self-similar solutions are possible only for the trivial case of the wave propagating exactly across the flow. The plane wave solutions have the form

$$u(x, y, t) = v(\eta, t), \qquad \eta = x\cos\theta(0) + y\left(\sin\theta(0) + \alpha t \cos\theta(0)\right), \tag{4}$$

The wave profile $v(\eta, t)$ obeys the (1+1)-dimensional PDE system

$$\frac{\partial v}{\partial t} = f(v) + K(t) D \frac{\partial^2 v}{\partial \eta^2}, \tag{5}$$

where the effective diffusion matrix $K(t)D$ is determined by scaling factor $K(t)$,

$$K(t) == 1 + 2\alpha t \cos\theta_0 \sin\theta_0 + \alpha^2 t^2 \cos^2\theta_0, \tag{6}$$

$\theta_0 = \theta(0)$, and $\theta(t)$ is the angle between the normal to the wavefront and the x-axis (or between the wavefront and the y-axis). In physical space, the dependence (6) corresponds to a change of the distance between isophase lines according to the equation (see Figure 1):

$$\lambda(t) = \lambda(0)(1 + 2\alpha t \cos\theta_0 \sin\theta_0 + \alpha^2 t^2 \cos^2\theta_0)^{-1/2}, \tag{7}$$

and the propagation angle at time t is

$$\theta(t) = \arctan(\tan(\theta_0) + \alpha t). \tag{8}$$

Thus, for plane waves, the problem reduces to that for propagation of excitation waves in a 1-dimensional cable, with diffusion depending explicitly on time. Now we consider the conditions under which this dependence can cause a propagation block, and hence a break in the wave.

3 Propagation block of a solitary wave

We assume the following properties of the unperturbed version of this equation $(K \equiv 1)$:

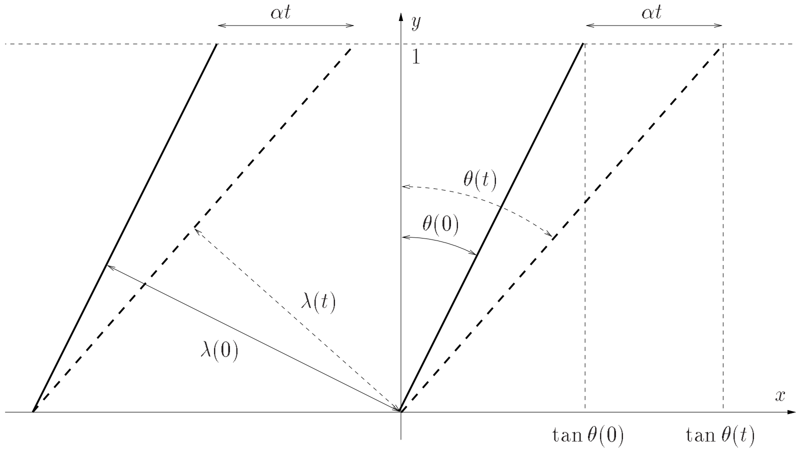

Figure 1: Schematic diagram of the plane wave deformation by the shear flow. Bold solid lines are equiphase lines at time moment 0, and bold dashed lines are the same lines at time moment t.

1. There exists a stable solitary wave solution $v(\eta, t) = V(\eta - c_v t)$, whose width $L = L_{\mathrm{norm}}$, is defined, for example, as the separation between points in which some component of v has a selected value.

2. This solitary wave can develop from initial conditions in the form of this same wave laterally squeezed, *i.e.* $v(\eta, 0) = V(k\eta)$, $k > 1$, with width, $L_{\mathrm{init}} = L_{\mathrm{norm}}/k$, shorter than normal but longer than some minimal width, $L_{\min}$ ($L_{\min} < L_{\mathrm{init}} < L_{\mathrm{norm}}$), but if $L_{\mathrm{init}} < L_{\min}$, the wave decays.

3. The typical time for development/establishment of the wave profile is τ_{prof}. If, as is often the case, the excitation waves are supported by processes of different time scales, then τ_{prof} will be the slowest of them (*i.e.* the time constant of the limiting stage). The significance of this parameter will emerge below.

If $K \neq 1$ but is any positive constant, then assumption 1 implies that (5) has a stationary solitary wave solution $v(\eta, t) = V(K^{-1/2}\eta - c_v t)$, with width $L_{\mathrm{stat}}(K) = L_{\mathrm{norm}} K^{1/2}$. If $K(t)$ is not constant but changes slowly, we may expect that the solution will have the same form as this wave, slowly adjusting its width accordingly. If $K(t)$ changes too rapidly, only then may the wave solution collapse.

With the assumptions listed above, we can formalise a phenomenological model. Let us assume, for simplicity, that the dynamics of the wave width is linear with a constant relaxation time τ_{prof}. As the instantaneous equilibrium state should change in accordance with $K(t)$, this gives

$$\dot{L} = \tau_{\mathrm{prof}}^{-1}\left(K^{1/2}(t) L_{\mathrm{norm}} - L\right), \qquad L(0) = L_{\mathrm{norm}}, \qquad L(t) \geq K^{1/2} L_{\min}\ \forall t; \tag{9}$$

This equation is in terms of the spatial variable η used in (5), which physically corresponds to the width measured in the direction of the flow. The rescaled width $\bar{L} = K^{-1/2}L$, corresponding to real width measured perpendicularly to the wavefront, then obeys

$$\dot{\bar{L}} = \tau_{\mathrm{prof}}^{-1}(L_{\mathrm{norm}} - \bar{L}) - \frac{\dot{K}}{2K}\bar{L}, \qquad \bar{L} \geq L_{\min}. \tag{10}$$

The starting and the final asymptotic value of $\bar{L}$ is L_{norm}. In between, it decreases below L_{norm} but always remains positive. The minimal value of $\bar{L}$ is achieved at $\dot{\bar{L}} = 0$ which gives

$$1 + \tau_{\text{prof}} \frac{\dot{K}}{2K} = \frac{L_{\text{norm}}}{L_{\text{min}}}. \tag{11}$$

The system of equations (9,11) determines, in principle, the critical shear α_* at which a break occurs and the corresponding time t_* of the break; however, the exact solution is rather tedious.

To obtain a simple analytical estimate, let us consider the case of practical interest, when the ratio of the excitation timescale to the recovery timescale is

$$\tau_{\text{exc}}/\tau_{\text{rec}} = \epsilon \ll 1. \tag{12}$$

Propagation of excitation waves in this limit is described by the Fife approximation [2]. In particular, the limiting stage of wave formation is establishment of its width, which happens on the time scale of $\tau_{\text{prof}} \propto \tau_{\text{rec}}$, and minimal possible width from which the wave can recover is of the order of the excitation front width, $L_{\text{min}} \propto c_v \tau_{\text{exc}}$, whereas, in contrast, the normal wave width is, obviously, $L_{\text{norm}} \propto c_v \tau_{\text{rec}}$.

In this limit we should expect that the breakup occurs only if the effective diffusivity changes very quickly compared with $\tau_{\text{prof}} = \tau_{\text{rec}}$. Assuming, in a self-consistent way, that $t_* \propto \tau_{\text{exc}}$ and neglecting the change of $L(t)$ during this time interval, $L(t) \approx L_{\text{norm}}$, to leading order we obtain a system:

$$L_{\text{norm}}/L_{\text{min}} = \epsilon^{-1} = K^{1/2} = \left(1 + \frac{\tau_{\text{prof}} \dot{K}}{2K}\right). \tag{13}$$

Using (6) in (13), $\tan\theta(t_*) \approx \alpha_* t_* \approx \epsilon^{-1}$, then (13) implies $\tau_{\text{prof}}/t_* \approx \epsilon^{-1}$, and so the solution is

$$\begin{aligned} t_* &\approx \epsilon \tau_{\text{prof}} = \tau_{\text{exc}}, \\ \theta(t_*) &\approx \pi/2 - \epsilon, \\ \alpha_* &\approx \tau_{\text{prof}}^{-1} \epsilon^{-2} = \frac{\tau_{\text{rec}}}{\tau_{\text{exc}}^2}, \end{aligned} \tag{14}$$

in agreement with the original assumptions. This result can also be substantiated by numerical simulation and by accurate asymptotic analysis of the phenomenological ODE model; this however is beyond the scope of this communication and will be published elsewhere.

Thus there is a *critical* shear, above which a solitary wave is quenched, and the value of this shear depends on the difference between the time scales of excitation and recovery processes, which is a measure of the excitability of the system; the more excitable the system, the greater the shear needed to destroy the wave.

4 Propagation block of periodic waves

For periodic wavetrains the situation is completely different, as the spatial period measured in terms of the variable η (the period in the direction of the flow) is fixed. In physical space, if measured in the instantaneous direction of propagation, the spatial period changes according to (7). But in excitable media, there is always a minimal wavelength, λ_* at which a periodic wavetrain can propagate, and so $\lambda(t)$ decreasing below this value is a sufficient condition for the propagation block. From (7) we obtain the following estimate of the time and the angle for which the break will occur, for any value of the shear however small:

$$\theta_*^0 = \arctan(1/k), \quad t_* = \alpha^{-1}(k - 1/k), \quad \theta(t_*) = \arctan(k), \tag{15}$$

where

$$k = \lambda(0)/\lambda_*. \tag{16}$$

5 Numerical illustrations

So far we have considered only plane waves. To verify the estimates and analyse the effect of the shear flow on more complicated autowave patterns, we have performed numerical simulations for the FitzHugh-Nagumo system with the flow incorporated, in the following form

$$\begin{aligned} \frac{\partial E}{\partial t} &= c_1 E(E-a)(1-E) - g + \alpha y \frac{\partial E}{\partial x} + D\nabla^2 E, \\ \frac{\partial g}{\partial t} &= \epsilon(c_2 E - g) + \alpha y \frac{\partial g}{\partial x} + \delta D \nabla^2 g. \end{aligned} \tag{17}$$

We shall refer to the space and time units of this equation as s.u. and t.u. respectively. The parameter values were chosen $c_1 = 10$, $a = 0.02$, $\epsilon = 0.1$, $c_2 = 5$, $\delta = 1$ and $D = 1$. We solved this system with an explicit Euler scheme (forward time, centered space), with space step $h_s = 0.5$ s.u., in a rectangular medium $(x, y) \in [0, L] \times [-M/2, M/2]$ with periodic boundary conditions at $x = 0, L$ and non-flux boundary conditions at $y = \pm M/2$. The sizes of the medium, L and M, the velocity gradient, α, and the time step, h_t, were varied in different experiments. The minimum wavelength of a periodic train in medium with no shear ($\alpha = 0$) is 19.0t.u. and the wavelength of the spiral wave is 41.0s.u.

The evolution of a solitary plane wave is shown in Figure 2. The horizontally propagating wave was initiated in the medium with no shear and then the shear flow was switched on, which corresponds to the conditions of the analytical estimation. The excitation and recovery variables are E and g and their characteristic times are, respectively, $\tau_{\text{exc}} \propto 1$ t.u. and $\tau_{\text{rec}} \propto 1/\epsilon = 10$ t.u. According to (14), this means that $\alpha_* \propto 10$ t.u.$^{-1}$ for our choice of parameters. The threshold value of the velocity gradient necessary for breaking a single plane wave was found numerically to be $\alpha_* = 6$ t.u.$^{-1}$, the time $t_* = 1.5$ t.u. and the wave orientation at the moment of the break $\tan\theta(t_*) = 15$, which, to this order of magnitude, is consistent with the analytical estimates of (14), $\alpha_* = 10$ t.u.$^{-1}$, $t_* = 1$ t.u., and $\tan\theta(t_*) = 10$.

We have studied what happens to autowave structures at velocity gradients much less than this threshold. According to (15) and (16), we have for this medium $k \approx 2.16$, and at $\alpha = 0.06$ t.u.$^{-1}$ the wavebreak of the periodic train occurs at $t_* \approx 28$ t.u. at the angle of $\theta(t_*) \approx 1.14$ rad. These predictions, obtained for plane waves, agree, in order of magnitude, with simulations of the evolution of more complicated autowave patterns, the spiral wave and the target pattern.

Figure 3 illustrates the evolution of a series of topologically circular waves initiated by periodic stimulation of a point in the medium, with the period equal to the period of the spiral

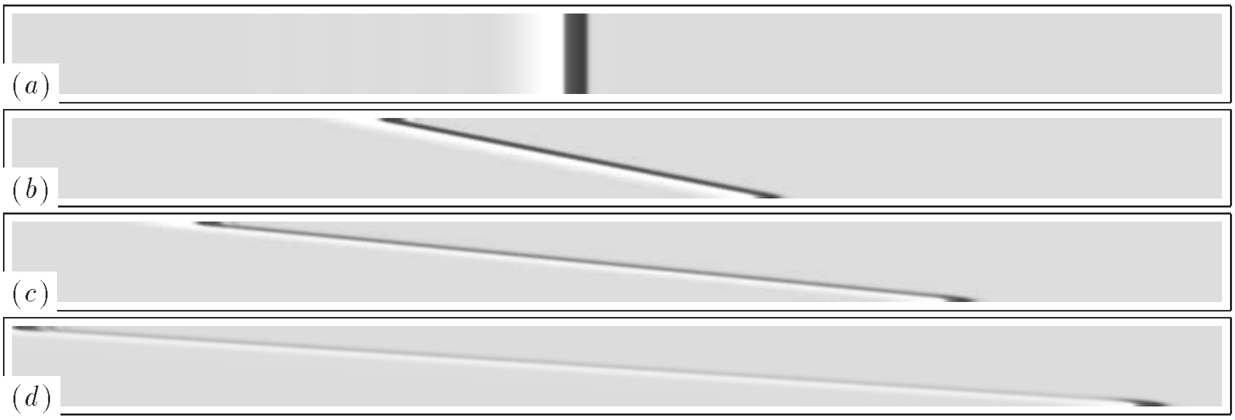

Figure 2: Conduction block of a solitary plane wave in the linear shear flow. Velocity gradient $\alpha = 10\,\mathrm{t.u.}^{-1}$, medium size $450\,\mathrm{s.u.} \times 30\,\mathrm{s.u.}$, time step $h_t = 5 \cdot 10^{-5}$ t.u. Shown are snapshots of the E field with interval 0.5 t.u.

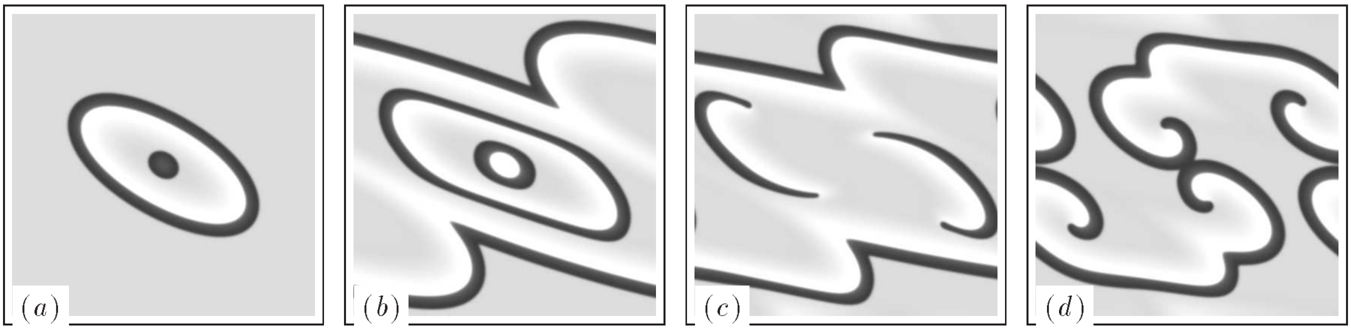

Figure 3: Breakup of a target pattern. Velocity gradient $\alpha = 0.06\,\mathrm{t.u.}^{-1}$, medium size $200\,\mathrm{s.u.} \times 200\,\mathrm{s.u.}$, time step $h_t = 5 \cdot 10^{-3}$ t.u. Shown are snapshots of the E field with interval 27 t.u.

wave. It can be seen that while the first wave propagates without problems, the propagation of the second is suppressed and the third wave is blocked. This block occurs not for the whole wave but at some points only, leading to wavebreaks which curl up into spirals. The first breaks occur to the third wave, at time $t \approx 63$ t.u., that is 19.4 t.u. after its initiation, and at a propagation angle of about $\theta \approx 1.3$ rad, in good correspondence with the theory.

Similar numerical experiment has been made with a spiral wave initiated in a medium with ($\alpha = 0$) and then the shear flow switched on. The spiral wave has broken, and the time ($t_* \approx 48$) and orientation of the wave ($\theta(t_*) = 1.3$ rad), same as in the previous example. The correspondence in this case would be better but for the phenomenon of "plasticity" of the excitation wave: as the process is non-stationary, the visual break-up happens later than the time at which conditions of stationary propagation are violated. This explanation was confirmed by numerical experiments when the flow was stopped before the wave broke, but after it would have happened according to the analytical estimate; the wave subsequently broke, despite the absence of the flow.

These two examples show that, at least for the particular model chosen, the conditions of the wavebreak are almost the same whatever the origin and shape of the pattern is, and the order of magnitude of the time required for the wavebreak agrees with the estimate (15) obtained for plane periodic waves based on quasi-stationary arguments.

When a spiral wave succumbs to wavebreaks, those develop into new spiral waves. Thus, in a linear shear flow a “chain reaction” of spiral wave births and deaths leads to a “frazzle gas” of excitation wavelets. The mechanism for generation of this “frazzle gas” is different from that described in [9]. As this mechanism requires only a finite deformation of the medium, we may expect that it can play its role not only in constant flows, but in a more wide variety of situations. If oceanic plankton dynamics are considered as an excitable medium then currents can influence their spatial dynamics.

6 Development of the frazzle gas

The phenomenon of the conduction block of periodic wavetrains has macroscopic consequences for the properties of large-scale two dimensional excitable media with shear flow. Since this conduction block is dependent on the orientation of the waves, in case of a complicated autowave pattern it will lead to breaks of some of the waves. In an excitable medium, the wavebreaks typically lead to the generation of spiral waves, which are sources of new periodic wavetrains. This leads to a “chain reaction” of the spiral wave births, shown on Figure 4.

A local finite initial perturbation of a resting medium with a shear flow has led to the transition of the whole medium into a turbulent-like state, the “frazzle gas”. To characterise quantitatively the frazzle gas solution, we counted the number of the wavebreaks, defined as intersections of the isolines $E = 0.2$ and $g = 0.48$. Some typical dependencies of this number on time, for different values of the velocity gradient α, are shown on Figure 5. These fluctuations in the number of breaks may be modelled as a stochastic process by a birth and death model, as in [10], [11].

As it can bee seen on Figure 4, the dynamics of the generation of the new wavebreaks, in this particular experimental setup, is determined, in the first instance, by two different processes: the growth of the “horseshoe” pattern, due to the revolution of the spiral waves, and the deformation of that pattern. Subsequently, development of secondary breaks further increases the density of the wavebreaks, until it reaches the state of the dynamic equilibrium, when the number of the new wavebreaks is balanced by the rate of the wavebreak annihilation. The resulting pattern depends on the value of the velocity gradient, see Figure 6.

The simple criterion of the wave break of section 4 can be used for a rough analytical estimate of the equilibrium density of spiral waves. First, let us estimate the typical distance between the spiral waves, as being of the same order of magnitude as the distance at which the first break in a spiral wave occurs. This is made up by some minimal distance, of the order of the spiral core, or spiral wavelength $\lambda_{\text{s.w.}}$, and the distance propagated by the spiral wave in the time before the breakup, which is $t_* \approx \alpha^{-1}(k_* - 1/k_*) \propto \alpha^{-1}$, as in our case the critical deformation $k_* = \lambda_{\min}/\lambda_{\text{s.w.}} \approx 2.16$, which is of the order of 1. The typical distance between the spiral waves in the frazzle gas can then expected to be

$$l_{\text{s.w.}} = \beta\lambda_{\text{s.w.}} + \gamma c_{\text{s.w.}}\alpha^{-1}. \tag{18}$$

where $c_{\text{s.w.}}$ is velocity of the spiral wave and β and γ are some dimensionless coefficients of

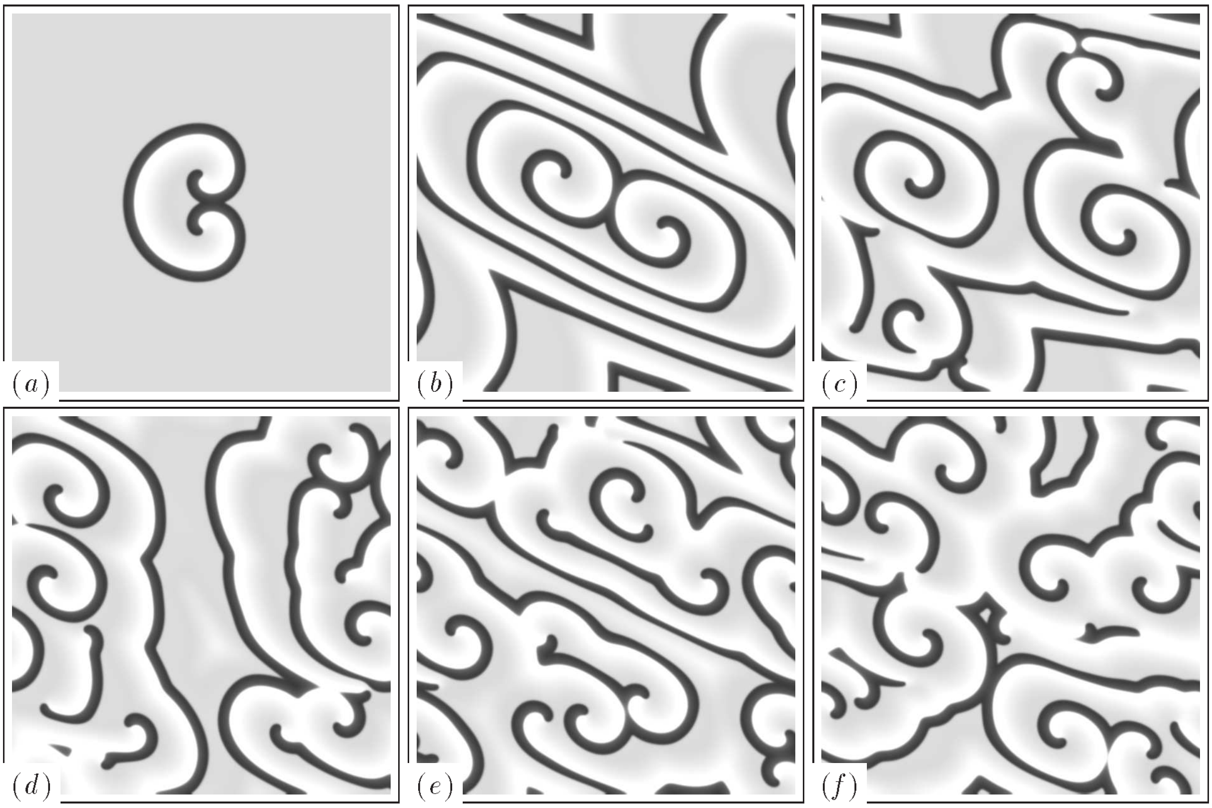

Figure 4: Development of a "frazzle gas" of spiral waves in linear shear flow. Shown are snapshots of E field in every 100 t.u., in a 300×300 s.u. medium, $\alpha = 0.02\,\mathrm{t.u.}^{-1}$.

the order of 1. The density of the spiral waves is then estimated by

$$\rho = \alpha^2/(K_1 + K_0\alpha)^2 \tag{19}$$

where

$$K_0 = \beta\lambda_{\mathrm{s.w.}}, \qquad K_1 = \gamma c_{\mathrm{s.w.}}. \tag{20}$$

As we mentioned above, in our model $\lambda_{\mathrm{s.w.}} \approx 19$ s.u. and $c_{\mathrm{s.w.}} = 1.8$ s.u./t.u.. Figure 7 shows the dependence $\rho(\alpha)$ found in numerical experiments, and the best fit by (19). This best fit is achieved with $K_0 \approx 36$ and $K_1 \approx 0.46$, which means $\beta \approx 1.9$ and $\gamma \approx 0.26$. Thus, the above consideration correctly describes the qualitative character of $\rho(\alpha)$ and order of magnitudes of corresponding coefficients. Recall that the estimates of section 4 also were only valid in the order of magnitude.

7 Discussion

Spiral and scroll waves in stationary excitable media act as organising centres: wavefronts from the rotating spiral wave propagate outwards, and the spiral acts as a source of high frequency, repetitive waves that eliminate by annihilation other patterns, leaving the spiral source to

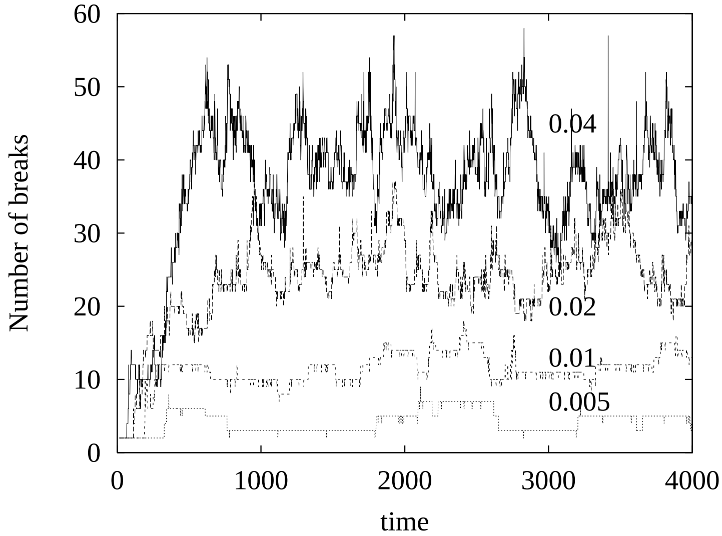

Figure 5: Number of wavebreaks as function of time, for velocity gradients $\alpha = 0.005$, 0.01, 0.02 and 0.04 t.u.$^{-1}$, in a 300×300 s.u. medium.

dominate the medium. Thus spiral and scroll patterns are often found in spatially extended, stationary excitable systems. Such patterns would simply be translated by a constant flow of the medium.

In section 4 we have shown that any linear shear can lead to wavebreaks in periodic wave trains, and we have illustrated this for periodic plane waves and target patterns, and for spiral wave sources. Thus spiral waves will not be stable in an excitable medium undergoing a linear shear flow. Once wave breakup has started, it continues and spreads through the medium, as each broken wave can act as a new source. This process continues until the medium is full of irregular wavebreaks, with a density that depends on the shear velocity gradient. Thus, in an excitable medium subject to shear flows we would expect the spatio-temporal irregularity of a frazzle gas behaviour to be observed.

A straightforward application is to moving chemical excitable media, e.g. Belousov-

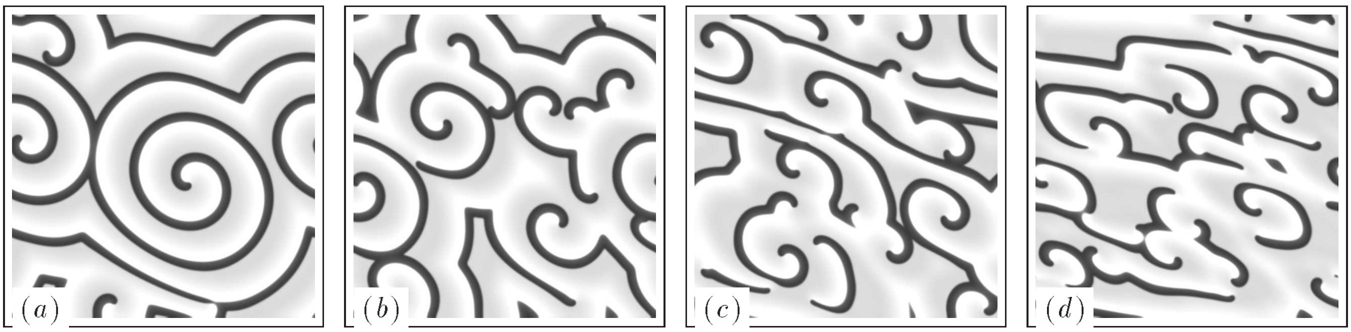

Figure 6: Structure of the "frazzle gas" of spiral waves (snapshots of the E field) at different velocity gradients: (a) 0.005 t.u.$^{-1}$, (b) 0.01 t.u.$^{-1}$, (c) 0.02 t.u.$^{-1}$ and (d) 0.04 t.u.$^{-1}$. Size of the medium 300×300 s.u.

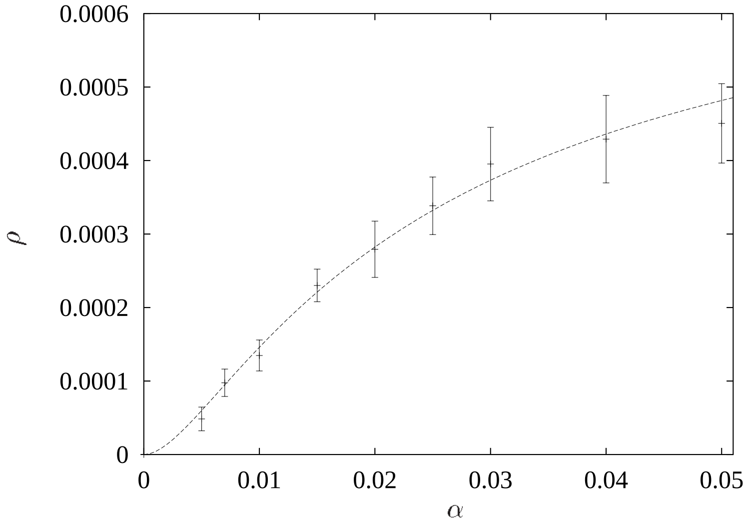

Figure 7: Time-average density of wavebreaks, ρ, for established "frazzle gas" state, as function of the velocity gradient, α, in a 300×300 s.u. medium. Points with error-bars show values obtained from simulation, the line shows the best fit to the theoretical dependence (19).

Zhabotinsky reaction. Effects of mechanical movement onto excitation patterns, including breakup of excitation waves, has been reported [12, 13]

One biological application is to plankton dynamics, where the shear flow represents the effects of currents. In the excitable medium model (3) the diffusion and advection terms are clearly separated. In chemical excitable media the diffusion term represents molecular diffusion, whereas in plankton dynamics models the diffusion represents turbulent mixing, and the advection term larger scale flows. Thus the space scaling that separates the diffusion from the advection in (3) for plankton dynamics does not separate biological from ocean space scales, but reflects the space scale of observation, with small space scales being treated as diffusion and larger space scales as flows. Thus conditions of the breaking of solitary and repetitive ways may be satisfied, depending on the chosen scale, which would create different patchiness structure at different scales. This qualitative prediction could be compared with observational (say, satellite) data on spatial and temporal spectra of plankton patchiness, where certain peculiarities would be observed on scales corresponding to characteristic times of phyto- and zooplankton growth.

In a quite different physical context, cardiac muscle is excitable and is moving [8]. Condition (14) assumes the finite deformation of the medium to happen on the time scale of the fast excitation processes, about 1 ms in cardiac muscle, which does not seem realistic. Therefore, any normal motion of the heart is highly unlikely to break the excitation wave in it. On the other hand, the condition for breaking of repetitive waves (15,16) only requires finite deformation of the medium during any time period. The critical deformation is the ratio of the spiral wave period and the refractory period, which is known to be quite close to unity in cardiac tissue. Thus, while unlikely to cause the first breaking, the medium motion may play its role (along with other suggested mechanisms, such as heterogeneity and anisotropy of tissue properties, instabilities of plane wave propagation and scroll wave shape etc.) in the development of fibrillation once the reentrant activity has started and before the muscle has lost contractility. Naturally, the motion of the cardiac tissue is far from being constant linear shear flow, and therefore the results can only be considered as hints to what could be expected in more realistic models of reentrant activity in the heart involving mechano-electric feedback.

Acknowledgements

This work has been supported by an equipment grant from the Wellcome Trust, and by grants EPSRC GR/L73364 and INTAS-96-2033.

References

[1] Holden, A.V., Markus, M. and H.G.Othmer (eds), *Nonlinear Wave Processes in Excitable Media*, Plenum, New York, 1991.

[2] Fife, P.C.: “Singular perturbation and wave front techniques in reaction-diffusion problems”, SIAM-AMS Proc., **10** (1976), 23–50.

[3] Truscott, J.E. and Brindley, J.: “Equilibria, stability and excitability in a general-class of plankton population-models” Phil. Trans. Roy. Soc. ser. A, **347** (1994), 703–718.

[4] Edwards, A.M. and Brindley, J.: “Oscillatory behaviour in a three-component plankton-population model” Dynamics and Stability of Systems, **11** (1996), 347–370.

[5] Truscott, J.E. and Brindley, J.: “Ocean plankton populations as excitable media”, Bull. Math. Biol., **56** (1994), 981–998.

[6] Coale K.H., Johnson K.S., Fitzwater S.E., Gordon R.M., Tanner S., Chauvez F.P., Ferioli L., Sakamoto C., Rogers P., Millero F., Steinberg P., Nightingale P., Cooper D., Cochlan W.P., Landry M.R., Constantinou J., Rollwagen G., Trasvina A. and Kudela R.: “A massive phytoplankton bloom induced by an ecosystem-scale iron fertilization experiment in the equatorial Pacific Ocean”, Nature, **383** (1996), 495–501.

[7] Pitchford, J.W. and Brindley, J. “Iron limitation, grazing pressure and oceanic HNLC regions”, submitted to J. Plankton Research, June 1998.

[8] Hunter, P.J., Nash, M.P. and Sands, G.B. “Computational electromechanics of the heart”, Chapter 12 in *Computational Biology of the Heart*, Holden, A.V. and Panfilov, A.V. (eds), J. Wiley & Sons, Chichester, 1997, pp. 345–409

[9] Markus, M., Kloss, G. and Kusch, I.: “Disordered Waves in a Homogeneous, Motionless Excitable Medium”, Nature, **371**(6496): 402–404, 1994.

[10] . Gil, L., Lega, J. and Meunier, J.L.: “Statistical properties of defect-mediated turbulence”, Phys. Rev. A, **41** (1990), 1138–1141.

[11] Hildebrand, M., Bar, M. and Eiswirth, M.: “Statistics of topological defects and spatiotemporal chaos in a reaction-diffusion system”, Phys. Rev. Lett., **75** (1995), 1503–1506.

[12] Winfree, A.T.: "Scroll-shaped waves of chemical activity in three dimensions", **181** (1973), 937–939.

[13] Agladze, K.I., Krinsky, V.I. and Pertsov, A.M.: "Chaos in the Non-Stirred Belousov Zhabotinsky Reaction is Induced by Interaction of Waves and Stationary Dissipative Structures", Nature, **308** (1984), 834–835.